Journal of University of Science and Technology Beijing
Volume 13, Number 6, December 2006, Page 564

Materials

Study on crystallization and microstructure of Li_2O-Al_2O_3-SiO_2 glass ceramics

Zhaoxia Hou[1,2], *Yongming Zhang*[3], *Huashan Zhang*[1], *Hongbo Zhang*[1], *Jing Shao*[1], *and Chunhui Su*[1]

1) School of Materials and Chemical Engineering, Changchun University of Science and Technology, Changchun 130022, China
2) Department of Chemical Engineering, Jilin Institute of Chemical Technology, Jilin 132022, China
3) Department of Material Science and Engineering, Shenyang Institute of Chemical Technology, Shenyang 110142, China
(Received 2006-02-08)

Abstract: Lithium aluminosilicate (LAS) glasses are generally difficult to prepare because of their high melting temperature. In this study, the preparation of LAS glasses was achieved at a relatively low melting temperature. The batch containing MgO-ZnO-Li_2O-Al_2O_3-SiO_2 was melted in a platinum crucible at 1550°C for 2 h and was then followed by two- or three-step heat treatment processes for nucleation and crystal growth. The characterizations were carried out by differential thermal analysis, X-ray diffraction, infrared spectroscopy, scanning electron microscopy, and UV-Vis-NIR scanning spectrophotometry. The hexagonal stuffed β-eucryptite solid solution crystallized at 840-960°C. Most of the hexagonal β-eucryptite solid solution transformed into the tetragonal β-spodumene solid solution at 1100°C. Almost all the aluminum atoms entered into the tetrahedral sites in the aluminosilicate network of the β-eucryptite/β-quartz solid solution. All of the Al atoms did not belong to the aluminosilicate network of the β-spodumene solid solution. The glass ceramic with a mean grain size of 10-20 nm is transparent, the transmittance reaches ~85% in the visible light wavelength.

Key words: inorganic compounds; glass ceramics; crystallization behavior; microstructure characterization

[*This work was financially supported by the Ministry of Education of China (No.KB20026).*]

1. Introduction

Glass ceramics have been defined as polycrystalline materials that are formed by controlled crystallization of suitable base glasses. The first glass ceramic produced industrially was introduced in the 1950s by Stookey [1]. The percentages of the glass and crystalline phases, as well as the crystal types, determine the properties of the glass ceramics. The basis of controlled internal crystallization lies in efficient nucleation, often enabled by a small amount of nucleating agent, which allows for the development of fine and randomly oriented grains in a ceramic, usually without voids, microcracks, or other porosity [2]. The most frequently used nucleating agents are TiO_2 and ZrO_2 oxides or their mixtures, which are more efficient according to Stewart [3]. Nuclei are formed and different crystalline phases grow in the glass matrix depending on the heat treatment processes.

These basic procedures have led to the rapid development of various glass ceramics. Since the 1960s, several studies on the crystallization and the microstructure evolution of Li_2O-Al_2O_3-SiO_2 (LAS) type glasses have been carried out [4-6]. The main crystalline phase in these glass ceramics consists of metastable solid solutions of the high quartz or keatite structure. Transparent and opaque glass ceramics based on the Li_2O-Al_2O_3-SiO_2 formulation have an exceptionally low, or even negative coefficient of thermal expansion (CET), and accordingly high thermal shock resistance, which determines that this kind of glass ceramics has potential to become a new generation of laser material.

LAS glasses are generally difficult to prepare because of their high melting temperature. It is very essential to study the synthesis process at a relatively low melting temperature because it is difficult to obtain glasses with excellent optical homogeneity at a very high melting temperature. In this study, the melting temperature was decreased by the introduction of certain additives. The crystallization behavior and microstructure of LAS glass ceramics are discussed.

2. Experimental

2.1. Preparation

The composition (wt%) of glasses is SiO_2, 55; Al_2O_3, 25; LiO_2+MgO+ZnO, 7; P_2O_5+CaO, 8.5; TiO_2, 3.5; Sb_2O_3, 1. Analytically pure SiO_2, Al_2O_3, ZnO,

Corresponding author: Chunhui Su, **E-mail:** sch@cust.edu.cn

$LiOH{\cdot}H_2O$, P_2O_5, CaO, $MgCO_3$, TiO_2, and Sb_2O_3 were used as the starting materials. TiO_2 and ZrO_2 were used as nucleating agents, and Sb_2O_3 was used as the clarifier. K_2O, MgO, ZnO, and P_2O_5 were added to reduce the viscosity [7]. Addition of P_2O_5 allowed for the production of highly homogeneous initial glasses and for the increase in the transmittance of glass ceramics, as compared with glass ceramics without P_2O_5 [8].

The batch was homogenized in the planetary ball mill (QM-1SP4, China) and then melted in a Pt crucible with stirring at 1550°C for 2 h in the $MoSi_2$ electrical resistance heating furnace having a PID temperature controller. The melt was then poured on a prewarmed stainless steel plate, the initial glasses were annealed at 530°C for 2 h and allowed to cool down to room temperature at a rate of 20°C/h to relieve internal stress. Finally, clear, transparent and bubble-free glasses were obtained.

2.2. Characterization

The nucleation and crystallization temperatures of the LAS glass were determined by differential thermal analysis (Pyris-Diamond, Perkin-Elmer, USA). The measurement was carried out with 10.286 mg of glass powder in an alumina crucible, under continuous nitrogen purging. The DTA curve was recorded in the range of 32-1275°C at a heating rate of 10°C/min. An X-ray powder diffraction system (D/max 2500 V, Rigaku, Japan) with Cu $K_{\alpha 1}$ radiation (0.154056 nm) was used and scanned from 5° to 70° at a scanning rate of 4°/min. SEM (S-4200, HITACHI, Japan) was used to study the morphology, the grain size, and the distribution of the glass ceramics in the residual glass matrix. The reorganization of the amorphous solid was confirmed by FT-IR spectroscopy (BRUKER Vertex 70 FT-IR), with a resolution of 4 cm^{-1}. The absorption spectra of the glass and glass ceramic samples were measured by UV-Vis-NIR scanning spectrophotometer (UV-3101PC, SHIMADZU, Japan). Before the transmittance measurement, specimens had been cut into blocks and polished to 10 mm×10 mm×1 mm disks. For the SEM observations, the disks were immersed in hot 80% phosphoric acid solutions for 15 min and then stopped etching in a rinsing bath (H_2O+acetone). The disks were coated with gold before SEM measurement.

3. Results and discussion

3.1. Differential thermal analysis (DTA)

The DTA curve of the LAS initial glass is shown in Fig. 1. There is an inapparent endothermic peak at 530°C, which indicates that the glass transformation is effected within a wide temperature range. The curve is characterized by two exothermic peaks at 767°C and 902°C, which correspond to the nucleation and crystallization temperatures, respectively. Also, there is a slight shoulder around 960°C that corresponded to the crystal transformation and will be verified by XRD analysis in the subsequent section.

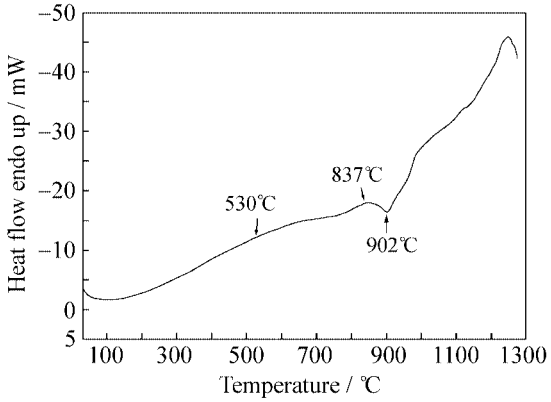

Fig. 1. DTA curve of the LAS base glass.

According to the DTA results, various heat treatment processes given in Table 1 were applied to study the nucleation and crystallization processes and the change of microstructure.

Table 1. Heat-treatment processes for glass samples

Samples No.	For nucleation	For crystallization
L_1	750°C×3 h	840°C×1.5 h
L_2	750°C×3 h	840°C×2 h
L_3	750°C×3 h	840°C×2 h+960°C×2 h
L_4	750°C×3 h	840°C×2 h+1100°C×2 h

3.2. XRD analysis

XRD patterns for some samples are shown in Fig. 2. The peaks corresponding to the major crystalline phase were marked with symbols. All the peaks were analyzed with the Joint Committee for Powder Diffraction Studies (JCPDS) cards. According to the XRD spectra of glass ceramics, L_1, L_2, L_3, and L_4, the amorphous contribution seems to be reduced. But the quantitative determination of the crystalline and amorphous phases is very difficult and it can only be stated that samples L_2, L_3, and L_4 are highly crystallized materials with a few residual glassy phases.

In comparison with standard samples, such as $Li_xAl_xSi_{1-x}O_2$ (40-0073) and $Li_xAl_xSi_{3-x}O_6$ (31-0707), the main crystalline phase of samples L_1, L_2, and L_3 has been identified as a β-quartz solid solution of $Li_2O{\cdot}Al_2O_3{\cdot}nSiO_2$ type, crystallized at 840-960°C. The high intensity and well-defined lines locate between 20° and 70°, namely (100), (101), (110), (200), (201), (112), (211), (212), and (203) planes. The crystal planes (110), (201), (212), and (200) have been select-

ed for determination of lattice parameters. The lattice parameters of the β-quartz solid solution have been calculated from the measured distance of crystal plane with the expression relative to the hexagonal crystal system [9]:

$$d_{hkl}^2 = \frac{a^2}{\frac{4}{3}(h^2+k^2+hk)+l^2\frac{a^2}{c^2}} \quad (1)$$

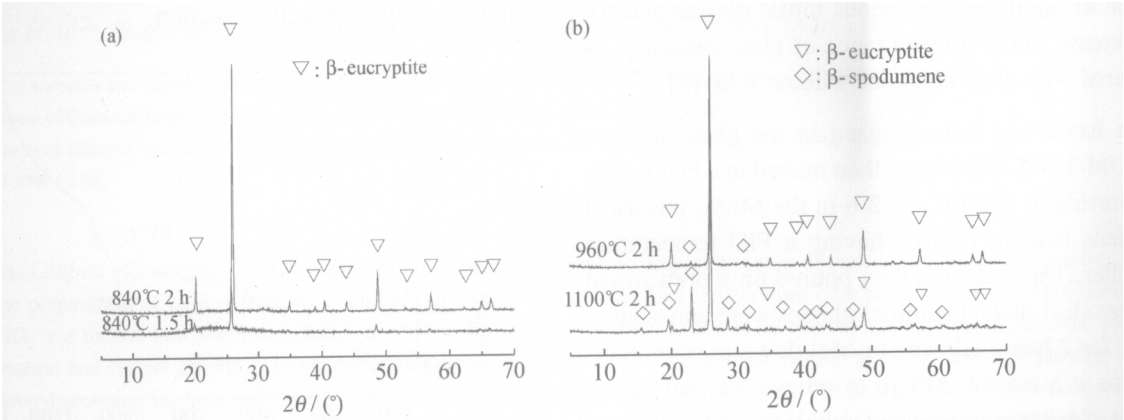

Fig. 2. Powder XRD patterns of LAS glass ceramics under different heat treatments: (a) L_1, L_2; (b) L_3, L_4.

The XRD data of L_2 are given in Table 2. L_2 is stuffed β-quartz solid solution with a hexagonal structure. Its mean values of the lattice parameters of the main crystalline phase are $a_e(L_2)$=0.5145(6) nm and $c_e(L_2)$=0.5475(4) nm. The *d*-spacings of JCPDS 40-0073 and JCPDS 21-503 are represented as $d_s(L_2)$ and $d_s(L_4)$ in Tables 2 and 3, respectively. The lattice parameters of β-quartz hexagonal structure in JCPDS 40-0073 are $a_s(L_2)$=0.5162 nm and $c_s(L_2)$=0.5456 nm. The lattice spacing of stuffed β-quartz solid solution has been calculated using $a_e(L_2)$ and $c_e(L_2)$ values obtained above, represented as $d_c(L_2)$. There is a good agreement between the calculated distance of crystal plane d_c and the experimental values $d_e(L_2)$ (see Table 2), which indicates that the lattice parameters $a_e(L_2)$ and the calculated $c_s(L_2)$ are correct. Here, subscript e represents experimental values, c represents calculated values, and s represents standard sample.

Table 2. XRD data relative to sample L_2

h	*k*	*l*	d_c (L_2) / nm	$d_s(L_2)$ / nm	$d_e(L_2)$ / nm
1	0	0	4.455	4.460	4.431
1	0	1	3.454	3.454	3.429
1	1	0	2.572	2.581	2.571
2	0	0	2.228	2.234	2.229
2	0	1	2.063	2.070	2.063
1	1	2	1.874	1.873	1.868
2	1	1	1.610	1.615	1.612
2	1	2	1.434	1.436	1.435
2	0	3	1.411	1.410	1.407

After further heat treatment for L_2 at 960°C for 2 h, sample L_3 was obtained. XRD patterns show the presence of β-spodumene solid solution, which indicates that the β-eucryptite solid solution begins to transform into the β-spodumene solid solution. And most of the β- eucryptite solid solution transforms into the β-spodumene solid solution after heat treatment at 1100°C for 2 h. Sample L_4 is very close to the $Li_{0.6}Al_{0.6}Si_{2.4}O_6$ (JCPDS 21-503). This is in conformity with the result obtained by Arnault *et al*. [8] and Ostertag *et al*. [10]. The well-defined lines locate between 40° and 70°, and the (333), (521) planes have been selected for the determination of lattice parameters. The lattice parameters of the tetragonal β-spodumene solid solution have been determined from the measured distance of crystal plane by the following formula [9]:

$$d_{hkl}^2 = \frac{a^2}{h^2+k^2+l^2\frac{a^2}{c^2}} \quad (2)$$

The lattice parameters calculated in this manner are $a_e(L_4)$=0.74836(3) nm and $c_e(L_4)$=0.90585(7) nm. The XRD data of L_4 is given in Table 3.

Table 3. XRD data relative to sample L_4

h	*k*	*l*	d_e (L_4) / nm	$d_s(L_4)$ / nm	$d_c(L_4)$ / nm
1	0	1	5.698	5.770	5.770
1	1	1	4.526	4.572	4.569
2	0	1	3.432	3.462	3.505
2	1	1	3.121	3.143	3.139
2	2	2	2.276	2.286	2.285
2	1	3	2.228	2.241	2.242
3	0	3	1.919	1.923	1.923
3	2	4	1.524	1.529	1.530
3	3	3	1.523	1.524	1.523
5	1	2	1.405	1.398	1.396
5	2	1	1.374	1.375	1.374
3	2	5	1.366	1.364	1.365

It can be seen that there is a little difference of the distance of crystal plane between the experimental and standard samples, which may be explained by the replacement of Li^+ ions by stuffed divalent Mg^{2+} and Zn^{2+} ions that have ionic radii of the same size order.

3.3. FT-IR spectroscopy analysis

Up to now, some infrared spectroscopy studies have been performed on glassy and crystallized materials of LAS systems [7, 11]. The main spectral features and difference between the base glass and glass ceramic specimens have been observed. However, the exact explanation of the infrared spectra is difficult because of the complexity of the material composition. The FT-IR spectra are shown in Fig. 3, it is similar to the study by Arnault *et al.*, which has a higher SiO_2 content (about 70wt%) [7].

As shown in Fig. 3, the IR spectra can be divided into two spectral ranges: the first one extends from 4000 to 1500 cm^{-1} and the second one from 1500 to 400 cm^{-1}. The high-frequency spectral range 4000-1500 cm^{-1} is identical for the four samples; they exhibit the same features: a wide band ~3423 cm^{-1} and a shoulder around 1600 cm^{-1} which are characteristic of the presence of molecular water probably in the batch composition. In this study, emphasis has been laid on the low frequency range 1500-400 cm^{-1} which is representative of the studied materials.

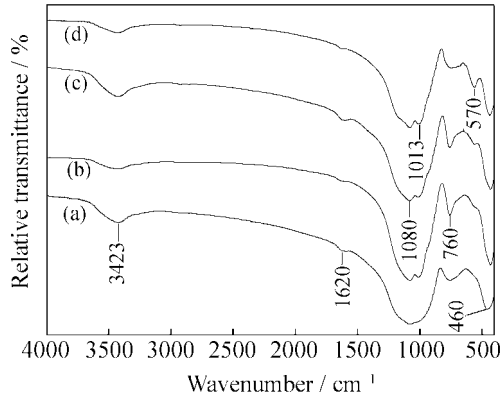

Fig. 3. FT-IR spectra of base glass and glass ceramic: (a) base glass; (b) L_2; (c) L_3; (d) L_4.

(1) Base glass.

The curve (a) shown in Fig. 3 is similar to the vitreous SiO_2 spectrum and shows three main absorption bands. The wide and strong band at 1080 cm^{-1} is the characteristic of the asymmetric stretching vibrations of Si–O–Si bonds in the silicates with three-dimensional network structure or in vitreous SiO_2. Aluminum is preferably located in the tetrahedral network and acts as network similar to silicon. Thus, it is likely that this band is attributed to the asymmetric stretching vibrations of Si–O–Al bonds. The band around 460 cm^{-1} is attributed to the O–Si–O bending vibrations, which is the characteristic band of the three-dimensional network silicate glasses. It can also be due to the symmetric stretching vibrations of LiO_4 tetrahedra and MgO_6 octahedra, which generally appear in this frequency range [12]. The weak band between 800 and 700 cm^{-1} corresponds to the symmetric stretching vibrations of Si–O–Si bonds, which appears at the same frequency for the vitreous silica. There is no absorption band near 950 cm^{-1}, which suggests that there is no nonbridging oxygen in the base glass [12]. This would confirm that Al atoms are tetra-coordinated. If the Al atoms act as modifiers, they would be hexa-coordinated Al^{3+} ions, which would be characterized by the presence of a band around 550 cm^{-1}; however, this band does not appear in the glass spectrum. It seems that the base glass is composed of a three-dimensional alumino-silicate network, where SiO_4 and AlO_4 tetrahedra are more or less uniformly distributed. The alkali and earth-alkali ions incorporate into the cavities and act as charge balancers compensating for the negative charge due to the substitution of Si by Al.

(2) Glass ceramics.

The curves (b), (c), and (d) given in Fig. 3 show a spectral change in comparison to the base glass spectrum. The spectral band at 1080 cm^{-1} splits into two spectra bands, ~1080 and ~1013 cm^{-1}. The high-frequency band at 1080 cm^{-1} is assigned to the stretching vibrations of Si–O–Si bonds, which is the characteristic of the tectosilicates. The frequency band at 1013 cm^{-1} is attributed to the asymmetric vibration of Si–O–Al bonds. A slight shoulder observed near 950 cm^{-1} is linked to the $Si–O^-$ vibration mode. Therefore, it seems that there are nonbridging oxygen ions in the residual vitreous phase of the glass ceramic L_2 and L_3. And a slighter shoulder can be observed in specimen L_4, which indicates there are few nonbridging oxygen ions in the residual vitreous phase. The band 430 cm^{-1} is the second main characteristic band of tetra-coordinated Si and is assigned to the bending vibrations of O–Si–O bonds. But it is located at a lower frequency than the band of base glass (460 cm^{-1}). This maybe resulted from the lattice vibration that occurred at the low frequency. Another spectral difference between the glass and glass ceramics appears in the range of 500-820 cm^{-1}. Contrary to the glass spectrum, the band centered at 760 cm^{-1} becomes stronger and narrower, which is probably due to the symmetric vibrations of Si–O–(Si, Al) bonds. According to previous studies, this band exists in the spectra of β-eucryptite and in the β-eucryptite/β-quartz solid solution [13], and also appears in the β-spodumene, but this band is weaker, and therefore specimens L_2 and L_3 are of β-eucryptite/β-

quartz solid solution, and specimen L_4 is of β-spodumene solid solution structure, which is in line with the results of the study of XRD patterns. The band around 570 cm^{-1} could be assigned to the AlO_6 vibration groups, which generally show an absorption in this frequency range. For β-spodumene solid solution, the band at 570 cm^{-1} is more intense and better defined than β-eucryptite/β-quartz solid solution. It may be attributed to the vibrations of Al–O^- bonds. Thus, it is found that almost all of the aluminum atoms enter into the tetrahedral sites in the aluminosilicate network of the β-eucryptite/β-quartz solid solution, and there is only a little amount of hexa-coordinated Al ions in the residual vitreous phase for specimens L_2 and L_3. As for specimen L_4, all of the Al atoms do not belong to the aluminosilicate network of the tetragonal β-spodumene solid solution, and a considerable proportion is in 6-fold coordination of the residual glassy phase.

3.4. SEM analysis

The SEM images are shown in Fig. 4. The SEM image of specimen L_1 is shown in Fig. 4(a). It is composed of crystallites of approximately 10~20 nm. The very fine grain size and low crystallization percent (deduced from XRD) can explain its transparency (~85%). Specimen L_2 is composed of crystallites of approximately 3-5 μm and the grain size is very uniform. These crystals are generally conglomerated in clusters and the vitreous interstitial phase is relatively limited, as shown in Fig. 4 (b). Specimen L_2 is translucent because of its relatively large grain size and highly crystalline nature. The SEM image of specimen L_4 is shown in Fig. 4(c). The grains are much larger than those of specimen L_2 and have irregular shape, which leads to the opacity of specimen L_4. There is close intergranular contact and the residual glassy phase is not uniformly distributed between grains.

The comparison of SEM between specimens L_1, L_2, and L_4 shows the dramatic effect of crystallization and heat-treatment processes on the glass ceramic microstructures.

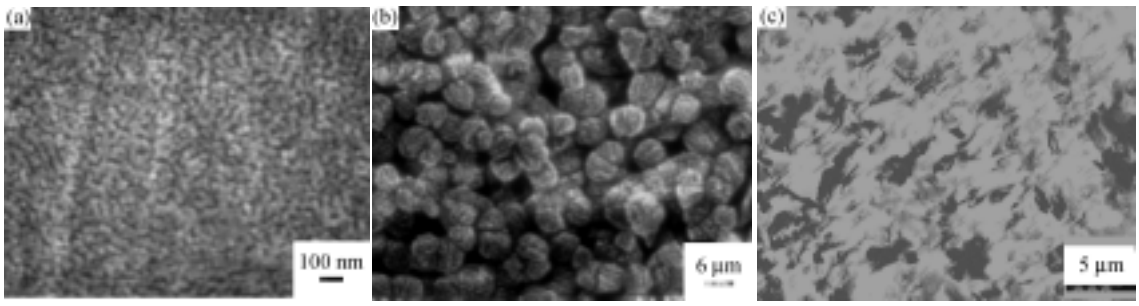

Fig. 4. SEM micrographs of LAS specimens L_1 (a), L_2 (b), and L_4 (c).

3.5. Transmittance analysis

The transmittance of the glass ceramic L_1 with a mean grain size of 10-20 nm is shown in Fig. 5. Nearly 85% in the visible light wavelength is reached.

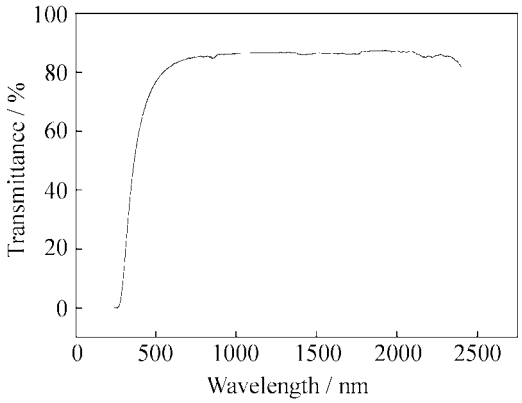

Fig. 5. UV-VIS-NIR spectroscopy for sample L_1.

4. Conclusions

Lithium aluminosilicate glasses containing MgO-ZnO-Li_2O-Al_2O_3-SiO_2 have been prepared by the conventional melting method at a relatively low temperature by introducing some additives, and subsequently converted to glass ceramics by controlled nucleation and crystallization processes. The hexagonal stuffed β-eucryptite/β-quartz solid solution of Li_2O-Al_2O_3-$nSiO_2$ type crystallized at 840-960°C. Most of the hexagonal β-eucryptite solid solution transforms into the tetragonal β-spodumene solid solution after heat treatment at 1100°C for 2 h. The lattice parameters of these two crystal phases have been calculated. There is a good agreement between the distance of crystal plane and the experimental value, indicating that the calculated lattice parameters are correct. Almost all the aluminum atoms enter into the tetrahedral sites in the aluminosilicate network of the β-eucryptite/β-quartz solid solution. All of the Al atoms do not belong to the aluminosilicate network of the tetragonal β-spodumene solid solution. The LAS glass ceramic with a mean grain size of 10-20 nm is transparent, and the transmittance is nearly 85% in the visible light wavelength.

References

[1] S.D. Stookey, *Photosensitively Opacifiable Glass*, US Pat-

ent, No.2684911, 1954.

[2] W. Höland and G. Beall, *Glass Ceramic Technology*, American Ceramic Society, USA, 2002, p.37.

[3] D.R. Stewart, TiO_2 and ZrO_2 as nucleants in a lithia aluminosilicate glass-ceramic, [in] L.L. Hench and S.W. Freiman eds. *Advances in Nucleation and Crystallization in Glasses*, Special Publication 5, American Ceramic Society, Columbus, 1971, p.83.

[4] G. H. Beall, B.R. Karstetter, and H.L. Rittler, Crystallization and chemical strength of stuffed β-quartz glass-ceramic, *J. Am. Ceram. Soc.,* 50(1967), p.67.

[5] A. Nordmann, Y.B. Bcheng, and A. Rivière, Microstructural study of two LAS-type glass-ceramics and their parent glass, *J. Mater. Sci.*, 32(1997), No.9, p.83.

[6] M. Mortier and D. Vivien, Ceramic and glass-ceramic lasers, *Ann. Chim. Sci. Mater.,* 28(2003), No.6, p.22.

[7] L . Arnault, M. Gerland, and A. Rivière, Microstructural study of two LAS-type glass-ceramic and their parent glass, *J. Mater Sci.,* 35(2000), No.9, p.2331.

[8] U.K. Kang, T.I. Chuvaeva, A.A. Onushchenko, *et al*., Radiative properties of Nd-doped transparent glass-ceramics in the lithium aluminosilicate system [J], *J. Non Cryst. Solids*, 278(2000), p.75.

[9] N.R. Yang, *Testing Methods for Inorganic Non-metal Materials* (in Chinese), Wuhan University of Technology, Wuhan, 1990, p.17.

[10] W. Ostertag, G.R. Fischer, and J.P. Williams, Thermal expansion of synthetic β-spodumene and β-spodumene silica solid solutions, *J. Am. Ceram. Soc.*, 51(1968), p.651.

[11] O.P. Girin, *The Structure of Glass*, Vol.3, Consultants Bureau, New York, 1964, p.105.

[12] P. Tarte, *Physics of Non-Crystalline Solids*, Wiley, New York, 1964, p.549.

[13] V.A. Florinskaya, E.V. Podushko, I.N. Gonek, *et al*., *The Structure of Glass*, Vol.3, Consultants Bureau, New York, 1964, p.96.